Numerical Modelling of Ground Faults in MV Networks for Reliable Testing of Protection Algorithms

Mirosław Lukowicz, Krzysztof Solak, Paweł Wicher, Bernard Wiecha
Institute of Electrical Power Engineering
Wroclaw University of Science and Technology
Poland, Wroclaw
email: miroslaw.lukowicz@pwr.edu.pl

Abstract— **The paper addresses the problems of digital modelling of MV networks with the focus on phenomena having a significant impact on the reliability of resulting data subsequently used for testing protection relays. In ATPDraw program the Ferranti current transformer (core-balance current transformer) model was developed that allows taking into account the composite error that is due to discrepancy of magnetic coupling between the cable cores and the secondary coil as well as to the magnetizing current of the transformer. The impact of higher harmonics in the supplying voltage on algorithm performance in pre- and fault conditions has been investigated as well. The test results obtained for data without mentioned disturbances have been compared with outcomes for faults in the system with current transformation errors and harmonics in the pre-fault MV network signals.**

Keywords—distribution grid; high impedance fault; mathematical programming

I. INTRODUCTION

The introduction into service of admittance criteria based protection relays solved the problem of selective detection of ground faults in MV networks regardless of the neutral point grounding mode. This statement applies to persistent faults via a relatively low fault resistance of approximately up to 5 kΩ and compensated networks equipped with the Active Neutral Current Forcing (ANCF) system. An open issue is still the difficulty in detecting of faults via high resistance (HIF), intermittent persistent ground faults and faults (low and high resistance) in compensated networks without or defective ANCF system.

The admittance criteria employed in MV feeder protection make use of fundamental component of zero sequence voltage and current measured on the secondary sides of those signals filters. We can point at two causes for the limited sensitivity of admittance protection, i.e. standing unbalance of the MV networks that is one of the determining factors governing fault detection sensitivity and errors of zero sequence current filters.

Since the fundamental role of overvoltage criterion U_0> is to activate admittance protections, its setting over the zero sequence voltage existing in the pre-fault state is a natural limitation for protection sensitivity in case of ground faults via relatively small fault resistances. Such faults do not result in sufficiently large increase of the zero sequence voltage and can even lead to its reduction in the consequence of the network symmetrization.

Another factor governing the reduction of the admittance protection sensitivity is the composite error of filters measuring the zero sequence currents in the protected lines. These errors have two separate sources. One results from the core magnetizing current and has a dominant role in the Holmgreen's CTs arrangement (it results from non-uniform magnetizing characteristics of three CTs' cores) and the second concerning Ferranti transformers results from unequal magnetical coupling between the primary windings (the phase conductors) and a secondary winding coiled on the magnetic core of CT.

It is given roughly in the literature on the MV feeder protection that these errors are larger in the Holmgreen CT arrangement and estimated to be up to 50 mA, whereas for Ferranti CTs to 25 mA (values associated with the secondary side of CT). Those values are referred to neither the load of the transmission line nor a current transformer ratio, what should be meant as they are reached in a practically permissible maximum line load. It is worth noting that in practice it is difficult to estimate the angle error for both the filters of the zero sequence current.

In the case of an ideal magnetic coupling between the primary circuits and the secondary circuit of Ferranti CT (e.g. IO-11 with a current ratio of 1: 100), the maximal error for small primary currents is not greater than 1 mA (secondary side) and occurs for the primary current of approximately 3 A. Those considerations obviously do not concern the saturation of the core for which the class and accuracy limit of CT specify the composite error.

Due to long-standing problem of limited sensitivity of admittance protections to HIF additional detection criteria are desirable. The conventional admittance based relays use only the fundamental components of the zero sequence voltage and current. New methods focus on making use of relationship between the arc fault on the feeder and characteristic high frequency components in the power system signals. In particular possibility of using them to discriminate between the faulty and

978-1-5090-5518-0/16/$31.00 ©2016 IEEE

healthy lines is the goal of investigations [1, 2, 3]. These frequency components have two generation mechanisms. They appear as harmonics and result from the nonlinear arcing in the faulty line or as interharmonics of transients dependent on the configuration and electrical parameters of the MV network.

The basic approach to analysis of relaying signals used to HIF detection in MV networks are filtration methods enabling estimation of the selected harmonic amplitude in the zero sequence current. In other approach Hilbert transform is used that goals to offset all frequency components of current or voltage by 90 degrees [4]. This transform makes possible to estimate the reactive power of the zero sequence signals in accordance with Budeanu theory on the basis of calculated instantaneous power of $3u_0$ and the transformed $3i_0$. In other approaches wavelet transform is used to analyze high-frequency components of relaying signals in terms of amplitude or phase relationships.

It should be mentioned that so far reported in the literature outcomes do not consider two sources of errors which according to the authors have the decisive impact on effectiveness of HIF detection methods or it is not given there explicitly. These are the harmonic distortion superimposed on relaying signals and the composite error of zero sequence current filters which need to be taken into account.

II. HIF Detection Method

In an insulated MV network the reactive power flow direction is the same for all high-frequency components (harmonics) in faulty line and it is of the opposite sign in healthy lines. The use of the total reactive power computed within a selected frequency band can be proposed to determine the faulty line. Starting from the definition of active power which equals the instantaneous electrical power averaged after fundamental period

$$P \overset{def}{=} \frac{1}{T}\int_0^T u(t)i(t)\mathrm{d}t \qquad (1)$$

we can use it to compute the reactive power according to Budeanu's theory, provided that all harmonic of current or voltage signal will be transformed in such a way that their amplitude are fixed, and phase changes about 90 degrees [4], that gives a formula for the reactive power [5]

$$Q \overset{def}{=} \frac{1}{T}\int_0^T u(t)i'(t)\mathrm{d}t \qquad (2)$$

where $i'(t)$ is instantaneous current after applied Hilbert transform.

In this approach the use of the mathematical programing without constraints is proposed to designing of a digital filter transforming the protection current signal ($3i_0$) in such a way to minimize the following objective function:

$$V(\mathbf{W}_m) = \frac{1}{2N_c N_s}\sum_{j=1}^{N_c}\sum_{n=1}^{N_s}\left[d_e(j,n,\mathbf{W}_m) - d_t(j,n)\right]^2 \qquad (3)$$

The objective function is the mean square error between the target d_t and the actual d_e instantaneous decision for a given training set. The value of this function at each step of the training changes only due to changes in the coefficients of the proposed algorithm

$$\mathbf{W}_m = \begin{bmatrix} W_0 & W_1 & W_2 & \cdots & W_{Nf} \end{bmatrix} \qquad (4)$$

where W_0 is the decisional threshold and other coefficients constitute a digital filter. Mean squared errors are computed over all training sequences, i.e. sampled current and voltage zero sequence signals measured in faulty line and other healthy lines.

The decision regarding the state of the line is made on the basis of averaged in the window of length N_{sr} instantaneous discrete in time power compared with the decisional threshold W_0. As a result, after applying a hyperbolic tangent decisional function

$$\mathrm{tansig}\,(x) = \frac{\mathrm{e}^{x} - \mathrm{e}^{-x}}{\mathrm{e}^{x} + \mathrm{e}^{-x}} \qquad (5)$$

we get a formula for the instantaneous decision

$$d_e(j,n,\mathbf{W}_m) = \\ = \mathrm{tansig}\left\{\frac{1}{N_{\mathrm{sr}}}\sum_{l=0}^{N_{\mathrm{sr}}-1}\left(\left[\sum_{k=0}^{N_{\mathrm{f}}-1} i(n-k-l)W_{k+1}\right]u(n-l)\right) + W_0\right\} \qquad (6)$$

where N_{sr} is the length of the averaging window of instantaneous power, N_f is the length of the window of the current filter, and $i(n)=3i_0(n)$, a $u(n)=3u_0(n)$.

On the basis of available training set of signal patterns and related decisional targets the training aiming in improving the bias and filter coefficients with respect to (3) was carried out. In the proposed approach the Levenberg-Marquardt optimization algorithm is used to evaluate necessary modifications of algorithm parameters as follows

$$\mathbf{W}_{m+1} = \mathbf{W}_m - \frac{\nabla V(\mathbf{W}_m)}{\mathrm{H}(\mathbf{W}_m) + \mu \mathrm{I}} \qquad (7)$$

where $\mathbf{W}_{m+1}$, $\mathbf{W}_m$ are sets of coefficients before and after the modification respectively, $\mathrm{H}(\mathbf{W}_m)$, is an approximation of Hessian, function $\nabla V(\mathbf{W}_m)$ is a gradient of V, I is an identity matrix, and μ is the control parameter weighting the solution between the steepest descent method (μ increases) and the Gauss-Newton method (μ decreases).

III. MV NETWORK MODEL

The optimization of coefficients **W** in the algorithm (4) and the appropriate tests were carried out using data from computer modeling of the insulated MV network described in [6]. Simplified diagram of the network is shown in Fig. 1. The model consists of five overhead cable lines in a radial layout with lengths from 12.5 km (F2) to 68 km (F1) supplying linear loads. Total capacitive network current and currents of individual lines are shown in Table 1, where I_{0i} is the ground fault current and I_{CFi} is the capacitive ground fault current of the protected feeder Fi, ϑ_{u0} and ϑ_{i0} are the ratios of zero sequence voltage and current transformers. Zero sequence line currents and the zero sequence busbars voltage are filtered using second order Butterworth analog filter and sampled with a 10 kHz frequency.

The model given in [6] was supplemented with two sources of interferences in relaying signals, i.e. non-uniform magnetic coupling between the primary (conductors of the cable) and the secondary winding of ground fault CTs, and the pre-fault harmonic distortion of the voltage source supplying the HV/MV substation.

A. Ferranti Current Transformer Model

Ferranti CT (core balanced) transformer can be modeled as either a single-phase four windings transformer (exact model) or as a Holmgreen arrangement of three ideal transformers supplying the fourth nonlinear CT of appropriate current transformation ratio. In this study the second method was chosen, as it simplifies the modeling of varied magnetic coupling (Fig. 2). The real ground fault CT IO-11 was modeled with the characteristic of the magnetizing branch given in Fig. 3. Assuming the expected secondary side current error I_μ under the maximum line load, the following formulas were derived for turns ratios of the ideal transformers in Holmgreen arrangement:

$$n_{L1} = 1 \tag{7a}$$

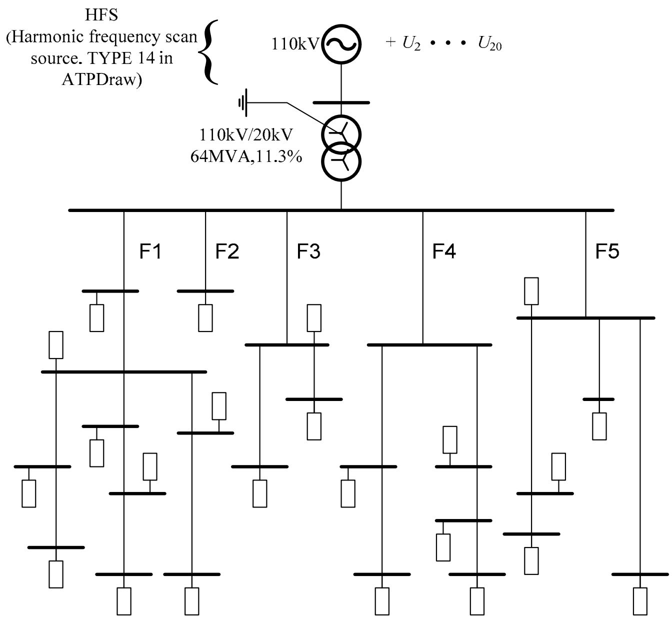

Fig. 1. Simplified diagram of the MV network

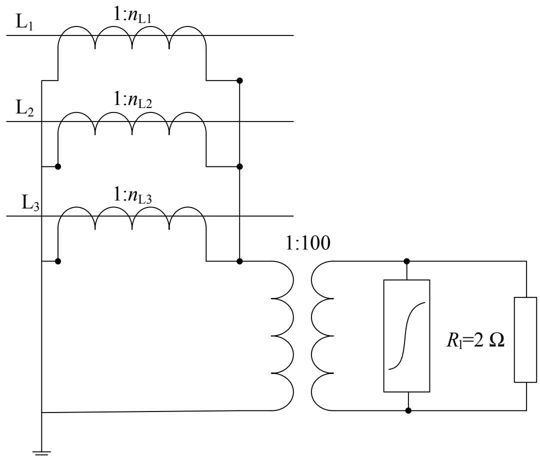

Fig. 2. Ground fault CT with the variable magnetic coupling of the primary conductors with the secondary side.

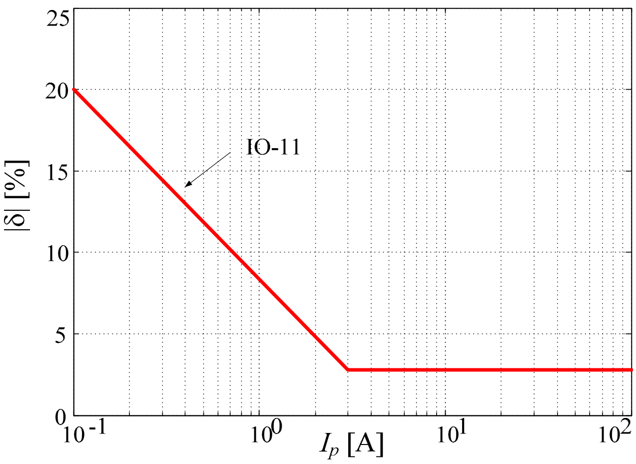

Fig. 3. Composite error of the ground-fault CT IO-11 vs. primary current.

$$n_{L2} = 1 + \frac{\vartheta_{i0} I_\mu}{I_N}\left(\frac{\sqrt{3}}{3}\sin\varphi - \cos\varphi\right) \tag{7b}$$

$$n_{L3} = 1 - \frac{\vartheta_{i0} I_\mu}{I_N}\left(\frac{\sqrt{3}}{3}\sin\varphi + \cos\varphi\right) \tag{7c}$$

where I_N is the pre-fault maximum expected load current of the feeder. It should be noted that the solution is not unique for the specified phase angle of the seeming zero sequence current on the secondary side of CT, so that one ideal transformer ration should be imposed, for example. $N_{L1} = 1$.

B. High frequency distortion modelling

The sources of harmonic distortion in the MV network signals can be modeled directly as the appropriate models of assumed non-linear loads, converters, etc. As the nature of the distortion in the network is unknown and it is not evaluated before relay installations the sources of distortions can be modeled on the aggregated basis. In the ATP-EMTP or ATPDraw there is a possibility of inclusion of additional voltage

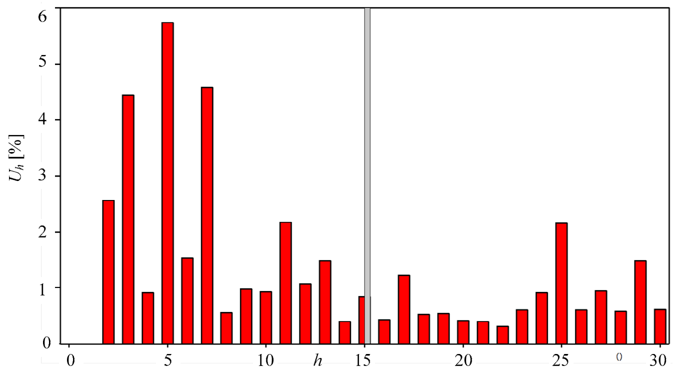

Fig. 4. Relative harmonic content in the phase voltage on the HV/MV substation busbar.

sources of the corresponding amplitudes, frequencies and phases to the source of the fundamental voltage. The harmonic amplitudes and HV\MV transformer impedance determine the impact of harmonic sources on phenomena in the MV network. In the study the worst case was assumed, i.e. maximal harmonic distortion was modeled as approved by Polish norms [7]. In such approach the source impedance for successive harmonics increases proportionally with the harmonic range. The selected rms voltage of harmonic sources are given in Table 2. As a result, the harmonic spectrum shown in Fig. 4 was determined from the phase voltage measured on the HV/MV substation busbar.

TABLE II. RMS VOLTAGE OF FUNDAMENTAL COMPONENT AND HIGHER HARMONIC SOURCES U_H IN 110 KV SYSTEM

h	1	2	3	4	5	6	7	8	9
***U* [kV]**	89.8	1.8	4.5	1.2	6.5	2.0	6.0	1.2	1.6
h	10	11	12	13	14	15	16	17	18
***U* [kV]**	1.2	4.0	2.0	3.0	1.2	2.0	1.2	2.0	3.0

C. Fault cases studied

To develop and analyze the proposed protection algorithm the zero sequence voltage and current waveforms recorded from modelling the MV system were initially sampled with 10 kHz frequency, and then down sampled to 5, 2, and 1 kHz. Only fault cases for which the conventional protections are not activated were selected to investigations, i.e. when $3U_0$> criterion with 10 V threshold set is not satisfied. The faults were HIFs based on the Hochrainer's arc model [6, 8, 9].

The testing and training sets have been divided into four subsets. Group MV_1 included fault cases from the network without sources of higher harmonics, MV_2 – signals distorted only by the harmonics, MV_3 - data from the network with real CTs and without sources of harmonics, MV_4 - faults in networks with both sources of interference of the relaying signals.

IV. RESULTS

The selected sets of signals were used to optimization of parameters **W** in the protection algorithm considered for various combinations of sampling frequencies 1, 2, 5, 10 kHz and averaging window length of ½, 1, 2, 3 fundamental cycles. We analyzed the algorithm performance only with respect to instantaneous decisions. We do not report the performance of algorithms with regard to fault cases, i.e. from the ignition of the arc to the final decision on the feeder condition. The final protection scheme should be completed with additional instantaneous decision counting and comparing units as well as delay units.

The results of the tests performed on the training and testing data with the selected sampling frequencies and lengths of the averaging window are summarized in Tables 4-7. It is readily seen that from 5 kHz frequency improvement of the optimization efficiency is no longer as dominant as after the change from 1 kHz to 2 kHz. Furthermore, the noticeable difficulty in optimization of the algorithm is observed for the cases from the set MV_3, and in particular from the set MV_4, i.e. for which both sources of disturbances were modelled.

Reliable investigations should take into account all possible system conditions, also those without the harmonic distortion and perfect transformation of ground fault CTs. Therefore, the optimization of the algorithm was carried out also for these data, i.e. for fault cases from sets MV_1 to MV_4 taken altogether. The appropriate training and testing results are summarized in Table III. As can be seen the selection of the suitable filter for the algorithm (4), which would have a satisfactory level of missing instantaneous decisions, is impossible. It should also be noticed that the operation of such an algorithm in the absence (disappearance) of pre-fault harmonics in the relying signals resulted in a degradation of its sensitivity.

V. CONCLUSION

This work has shown the significant impact of pre-fault disturbances in relaying signals on the dependability of new prospective algorithms protecting against HIFs in MV networks. Although the results are limited only to the selected protective relaying algorithm it is general in the sense that after optimization it may model e.g. wavelet transform or filtering of the arbitral frequency response. Therefore, one should expect that other types of algorithms, including the wavelet based detection methods, can show lower than expected sensitivity or give increased number of false trips when examined on data from the proposed fault model.

TABLE III FALSE AND MISSING INSTANTANEOUS HIF DETECTIONS FOR TRAINING AND TESTING PATTERNS FOR F_S = 5 KHZ(TRAINING BASED ON DATA FROM ALL DATA SETS)

TR -training	**TE - testing**	**N_{av} [samples]**	
MV	**Detections [%]**	**100**	
MV_{1234}	***false***	0.14	3.4
	missing	33.0	43.9
MV_1 /	***false***	0	0.1
	missing	57.0	56.0
MV_2 H	***false***	0	2.6
	missing	8.0	26.0
MV_3 PP	***false***	0.2	0.4
	missing	57.0	60.0
MV_4 H/CT	***false***	0.4	11
	missing	11.0	35.0

TABLE IV. FALSE AND FAILURE INSTANTANEOUS HIF DETECTIONS FOR TRAINING AND TESTING PATTERNS, F_S =1 KHZ

TR	**TE**	**N_{av} [samples]**							
MV	**Detections [%]**	**10**		**20**		**40**		**60**	
MV_1	***false***	0	0.1	0	0.08	0	0	0	0.1
/	***missing***	0	3.0	0	2.95	0	2.72	0	3.0
MV_2	***false***	0	0	0	0.1	0	0	0	0
H	***missing***	0.27	3.95	0	1.81	0	1.53	0	1.37
MV_3	***false***	0.54	0.63	0.16	0.53	0.16	0.6	0.06	0.6
PP	***missing***	25.8	30.0	13.6	12.9	13.2	13.1	10.65	12.6
SN_4	***false***	0.5	0.36	0.64	0.97	0.47	0.47	0.6	0.82
H/PP	***missing***	78.6	84.44	70.0	81.33	68.5	82.32	69.0	81.1

TABLE V. FALSE AND MISSING INSTANTANEOUS HIF DETECTIONS FOR TRAINING AND TESTING PATTERNS, f_s =2 KHZ

TR	**TE**	**N_{av} [samples]**							
MV	**Detections [%]**	**20**		**40**		**80**		**120**	
MV_1	***false***	0	0.15	0	0.17	0	0.6	0	0.1
/	***missing***	0	3.2	0	3.18	0	4.13	0	4.34
MV_2	***false***	0	0	0	0	0	0	0	0
H	***missing***	0.29	3.82	0	4.2	0	4.2	0	4.1
MV_3	***false***	0.73	1.12	0	1.21	0	1.4	0	1.28
PP	***missing***	10.82	12.0	0	7.01	0	5.74	0	5.63
MV_4	***false***	0.38	0.41	0.37	5.26	0	2.5	0.31	4.55
H/CT	***missing***	78.12	81.5	43.15	67.81	47.9	69.0	41.93	70.0

TABLE VI. FALSE AND MISSING INSTANTANEOUS HIF DETECTIONS FOR TRAINING AND TESTING PATTERNS, f_s == 5 KHZ

TR	**TE**	**N_{av} [samples]**							
MV	**Detections [%]**	**50**		**100**		**200**		**300**	
MV_1	***false***	0	0.3	0	0.2	0	0.1	0	0.2
/	***missing***	0	3.0	0	3.2	0	5.8	0	1.9
MV_2	***false***	0	0	0	2.1	0	2.24	0	2.35
H	***missing***	0.24	4.3	0	18.9	0	20.0	0	19.9
MV_3	***false***	0.27	0.53	0	1.28	0	1.6	0	1.3
PP	***missing***	4.55	7.8	0	7.2	0	5.8	0	4.8
MV_4	***false***	0.38	0.4	0	5.3	0	7.37	0	7.7
H/CT	***missing***	69.9	75.4	2.74	41.9	0	45.87	0	46.1

TABLE VII. FALSE AND MISSING INSTANTANEOUS HIF DETECTIONS FOR TRAINING AND TESTING PATTERNS, f_s =10 KHZ

TR	**TE**	**N_{av} [samples]**							
MV	**Detections [%]**	**100**		**200**		**400**		**600**	
MV_1	***false***	0	0.15	0	0.5	0.03	0.7	0	1.0
/	***missing***	0	3.2	0	3.2	0.24	6.6	0.04	3.5
MV_2	***false***	0	0	0	2.2	0	2.4	0	3.7
H	***missing***	0.29	4.4	0	26.2	0	25.0	0	29.7
MV_3	***false***	0.25	0.53	0	0.6	0	1.9	0	1.4
PP	***missing***	4.84	5.7	0	8.8	0	8.6	0	4.0
MV_4	***false***	0.5	0.53	0	8.6	0	10.1	0	9.0
H/CT	***missing***	66.9	73.5	0	50.4	0	49.6	0	46.2

REFERENCES

[1] Marciniak L., “Identyfikacja zwarć doziemnych wysokorezystancyjnych w sieciach średnich napięć”, Przegląd Elektrotechniczny”, ISSN 0033-2097, R. 91 NR 8/2015.

[2] Kwon W. H., Lee G. W., Park Y. M., Yoon M.C. and Yoo M. H., “High Impedance Fault Detection Utilizing Incremental Variance of Normalized Even Order Harmonic Power”, IEEE Trans. on Power Delivery, Vol. 6, No. 2, April 1991.

[3] Aucoin B. M., Russel B. D., “Distribution high impedance fault detection using high frequency current components”, IEEE Trans. Power Apparatus System, vol. PAS-101, No. 6, pp. 1596-1606, June 1982.

[4] Tao Cui, Xinzhou Dong, Zhiqian Bo ;Juszczyk A., “Hilbert-Transform-Based Transient/Intermittent Earth Fault Detection in Noneffectively Grounded Distribution Systems”, IEEE Trans. on Power Delivery, Vol. 26, No. 1, Jan. 2001.

[5] L. S. Czarnecki, “Wspomnienie o Profesorze Stanisławie Fryzem I refleksje nad Jego miejscem w teorii mocy”, Przegląd Elektrotechniczny”, ISSN 0033-2097, R. 87 NR 1/2011.

[6] M. Lukowicz, B. Wiecha, P. Wicher, “Application of optimization techniques in development of new protection algorithms for MV distribution feeders”, 12th IET International Conference on Developments in Power System Protection (DPSP 2014), Copenhagen, 31 March – 3 April 2014.

[7] PN-EN 50160:2002 Parametry napięcia zasilającego w publicznych sieciach rozdzielczych, s. 13-15, ISBN 83- 236-2376-7.

[8] Emanuel A. E., Cyganski D., Orr J. A., Shiller S., Gulachenski E. M.: „High impedance fault arcing on sandy soil in 15kV distribution feeders: contribution to the evaluation of the low frequency spectrum”, IEEE Trans. Power Delivery, vol. 5, No. 2, pp. 676-686, April 1990.

[9] Kizilcay M., Pniok T.: „Digital System Simulation of Fault Arcs in Power Systems”, ETEP, Vol. 1, No. 1, Jan/Feb. 1991, pp. 55–60.